4/16-190

CONTRACTOR REPORT

SAND89—7096
Unlimited Release
UC—722

Evaluation of Material Homogeniety as a Function of Thickness of Low-Alloy Ferritic Steel

T. L. Anderson, M. A. Lambert
Texas A&M Research Foundation
PO Box 3578
College Station, TX 77843

Prepared by Sandia National Laboratories Albuquerque, New Mexico 87185
and Livermore, California 94550 for the United States Department of Energy
under Contract DE-AC04-76DP00789

Printed November 1989

Issued by Sandia National Laboratories, operated for the United States Department of Energy by Sandia Corporation.

Available to DOE and DOE contractors from
Office of Scientific and Technical Information
PO Box 62
Oak Ridge, TN 37831

Prices available from (615) 576-8401, FTS 626-8401

Available to the public from
National Technical Information Service
US Department of Commerce
5285 Port Royal Rd
Springfield, VA 22161

NTIS price codes
Printed copy: A03
Microfiche copy: A01

SAND--89-7096

DE90 008069

EVALUATION OF MATERIAL HOMOGENIETY AS A FUNCTION OF THICKNESS OF LOW-ALLOY FERRITIC STEEL

Final Report

NOVEMBER 1989

Prepared by

TEXAS A&M RESEARCH FOUNDATION
P.O. Box 3578
College Station, Texas 77843

Principal Investigator
T.L. Anderson

Graduate Research Assistant
M.A. Lambert

Prepared for

SANDIA NATIONAL LABORATORIES
Albuquerque, New Mexico

EXECUTIVE SUMMARY

A series of Charpy and nil-ductility transition temperature (NDTT) tests were performed on 8 in and 12 in thick forgings of A508-4A, A508-4B, and A350-LF3 steels. Three different positions in thickness were tested in the 12 in forgings, while two locations in the 8 in forging were analyzed. Chemical analysis and metallographic examination were also performed on each material and in each thickness location.

The material toughness tended to be lower in the thicker forgings and in the center of a given forging. Low relative toughness coincided with well tempered microstructures, where equiaxed ferrite grains had begun to form. These grains are coarser than the packet structure that existed at earlier stages of tempering. Low quench rates (associated with thick sections and central regions of a given thickness) apparently accelerated the structural changes during tempering, which led to coarser microstructures with low toughness.

The NDTT results were suspect because most arrests occurred in the heat affected zones (HAZs) of the welds rather than in the parent metal. The measured NDTT values were lower than expected, based on published empirical correlations with Charpy energy. This was particularly true for the A508-4A steel. This provided further evidence that the drop weight tests were actually measuring the arrest properties of the HAZ in most cases. The fact that NDTT values were lower than expected is particularly surprising since the anvil test fixture was machined with a deflection stop 25 percent higher than the standard value.

INTRODUCTION

The United States Nuclear Regulatory Commission (NRC) has drafted guidelines for the fracture toughness of ferrtic steels for nuclear waste shipping containers(1). These draft guidelines specify extremely low nil-ductility transition temperature (NDTT) levels, ranging from -120 °F for A350-LF3 steel to -158 °F for A508-4A steel. However, the guidelines do not specify where the test specimens should be extracted when a thick section is being evaluated. The toughness could vary significantly through the thickness of a heavy section.

Sandia National Laboratories has asked Texas A&M University to evaluate the effect of position in thickness on the mechanical properties and microstructure of several materials. This report summarizes the results of this study.

TEST MATERIALS

Three low-alloy steels in two thicknesses were obtained for this investigation. A total of six forgings were tested. Table 1 lists the materials and thicknesses, together with the tensile properties as reported on the mill sheets. All four of the A508 class 4 forgings were (according to the steel mill) fabricated from the same ingot. Part of the ingot was forged to 9 in thickness and another section was forged to 13 in. Half of each section was then heat treated to the 4A specification while the other half was heat treated to the 4B standard. The forgings were then rough machined down to their final thicknesses of 8 and 12 in. Both of the A350-LF3 forgings were fabricated from a single ingot. Sections of the ingot were forged to 9 and 13 in, heat treated, and rough machined to the final thickness.

Test specimens were extracted from various locations within each forging, as illustrated in Fig. 1. Planes A and B correspond to locations within the 8 in forgings while planes C, D and E correspond to the 12 in forgings. This convention will be followed throughout this report.

TEST PROCEDURES

Drop weight testing, Charpy impact testing, chemical analysis, and metallographic examination were conducted on material from each of the five planes in each steel (see Table 1 and Fig. 1). The procedures are outlined briefly below. Experimental results are summarized in the sections which follow.

Drop weight tests were performed on 0.75 in thick P2 specimens. In most cases, the guidelines in ASTM Standard E 208-87 were strictly followed. However, the anvil test fixture was inadvertently machined with a 0.075 in

deflection stop rather than the required 0.060in. Thus the test fixture actually conformed to the P3 requirements, where the test specimens are 0.62 in thick. This error was not discovered until testing was completed Eight specimens were extracted from each thickness plane. Initial tests at room temperature confirmed that the welds were sufficiently brittle to initiate fracture upon application of the impact load. The wax pencil/masking tape technique outlined in E 208 was used in all tests to verify contact of each specimen with the anvil stop block. Low test temperatures were obtained by spraying vaporized liquid nitrogen into an insulated chamber. Two thermocouples were mounted on each specimen; one on the surface and one approximately 0.5 in below the surface. (The hole for the thermocouple was drilled at one end of the specimen, well away from the weld bead.) When the surface and interior of a specimen reached the desired temperature, the specimen was quickly removed from the chamber and placed on the anvil in the drop tower where it was tested. The result was then recorded as either a break, no break or no test, as defined by E 208. Some of the "no break" specimens were heat tinted and then broken at low temperatures to observe the extent of the arrested brittle fracture.

Charpy impact testing was performed in accordance with ASTM Standard E 23-86. Low test temperatures were obtained by a cooling bath equipped with a temperature controller and an automatic stirrer. This cooling bath was used down to -130 °F. For lower temperatures, a nitrogen vapor system was used, similar to that used for the drop weight tests. The Charpy testing machine has a maximum available energy of 120 ft-lb. Most of the materials tested, however, had upper shelf toughness in excess of 120 ft-lb. Consequently, many of the specimens tested on the upper shelf did not fracture completely and we were unable to obtain accurate estimates of upper shelf toughness in many cases.

Small coupons were sent to Materials Analysis, Inc. in Dallas for chemical analysis. They utilized an ARL 3520 series quantometer and a Leco IR 12 Carbon Determinator. The coupons were extracted from broken drop weight specimens. Each material and thickness plane (Fig. 1) was analyzed.

Additional coupons were obtained from each material and thickness position for metallographic examination. Specimens were mounted in a thermoseting plastic and prepared on automatic grinding and polishing equipment. The polished specimens were then etched in a Nital solution and observed in a Nikon Ephiphot metallograph. Photomicrographs were taken at 400 times magnification. Where possible, the ferrite grain size was measured by the linear intercept method.

CHEMICAL ANALYSIS

The results of the chemical analysis are given in Tables 2a to 2c. For each forging, the analysis for planes A to E are listed, together with the analysis reported by the vendor, and the ASTM specifications for that particular steel.

The Materials Analysis results are subject to ± 5 percent variation. The variation in composition with thickness location is within this margin for all three materials. Thus, there appears to be no significant variation in chemical composition with position in thickness.

In the case of the two A508-4B forgings (Table 2b), the analysis performed by Materials Analysis, Inc. indicates lower Cr and Mn than was reported by Jorgensen Steel. If the former analysis is accurate, the Cr and Mn contents are below the minimum allowable levels specified in ASTM A508. The reported Mn content is only slightly below the 0.20 percent requirement but the Cr content is significantly below the 1.50 percent required by the standard. The vendor reported very low S levels (0.001 percent) in the A 508 forgings. However, Materials Analysis Inc. was unable to verify this because their equipment had a minimum sensitivity of 0.01 percent.

The Cr and Mn content of the A508-4A forgings (Table 2a), as reported by Materials Analysis, Inc., is on the borderline of acceptability. The 4A and 4B forgings supposedly came from the same heat. However, the 4A forgings have significantly higher Cr than the 4B forgings (1.5 versus 1.2 percent). The Mn content of the 4A forgings is slightly higher than that of the 4B forgings. The reported amounts of the other elements are virtually identical. Either the 4A and 4B forgings did not come from the same heat as reported by the vendor, or the 4B forging somehow lost 0.3 percent Cr during heat treatment. The latter explanation seems unlikely.

The results could not have been influenced by bias on the part of Materials Analysis. They were provided with 15 numbered samples for analysis. They were not told the alloy designation, nor were they provided with the mill analyses for any of the materials. The fact that the results for a given material are consistent with thickness location indicates that their methods were consistent. Thus, the differences between the 4A and 4B forgings are real, not a result of experimental error.

NDTT RESULTS

The nil-ductility transition temperature data are summarized in Table 3. The results of individual tests are reported in Tables 4a to 4c. As stated earlier, the deflection stop was 0.075 in rather than the 0.060 in required for this thickness. This means that there was 25% more available energy in a given test than

would have been present in a normal P2 test. Thus the reported NDTT values are probably slightly higher than would have been the case had the standard deflection stop been used.

The NDTT values for the A 508 class 4 forgings are quite low. These materials would be acceptable according to the draft NRC guidelines(1). The center of each forging typically has an NDTT 20°F higher than the outer regions. This difference is barely significant, given the variability in the drop weight test.

The A350-LF3 forgings have NDTT values that are too high to be acceptable. In addition, the 12 in thick forging appears to be significantly more brittle than the 8 in thick forging in this material. The NDTT values would have been slightly lower had the standard deflection stop been used. However, the values would have almost certainly still been well above the -120 °F requirement for this material(1).

A number of the "no break" specimens were heat tinted and fractured at low temperatures. Most of these specimens indicated that the weld cracks actually arrested in the heat affected zone (HAZ). A specimen would usually fail completely when the crack propagated into the parent metal. In only a few cases (in the A508-4B material) did a crack arrest in the parent metal. Thus we may have actually measured the NDTT for the weld HAZ in many instances rather than the intended microstructure.

The weld beads were prepared precisely according to the guidelines in ASTM E 208-87. The welder used the consumable recommended by the Standard and made a single, continuous pass, started well away from the notch location. The weld itself was brittle, as proven by room temperature tests. Apparently, these materials produce extremely tough HAZs when welded.

CHARPY RESULTS

The Charpy data for all six forgings are plotted in Figs. 2 to 7. These data are tabulated in Tables 5a to 5c. The NDTT values from Table 3 are denoted by arrows on Figs. 2 to 7. Again, the thickness locations (Planes A, B, C, etc.) are as defined in Fig. 1.

The Charpy results seem to be more sensitive to thickness position than the NDTT results. For example, Fig. 2 indicates a shift of approximately 100 °F between planes A & B in the A508-4A steel, while the NDTT values are only shifted by 40 F. In all cases, the center planes (A and C) have higher transition temperatures than the outer planes.

The Charpy results for the A350-LF3 forgings indicate relatively high transition temperatures, which is consistent with the NDTT results. The 12

in thick A350-LF3 forging has lower CVN toughness than the 8 in forging, which is also consistent with the results in Table 3.

As stated in the *Test Procedures*, the Charpy testing machine has an energy capacity of only 120 ft-lb. Thus most of the values at or near 120 ft-lb in Figs 2 to 7 and Tables 5a to 5c do not reflect the true toughness of the material, because the hammer stopped without completely breaking the specimen in these tests. It was possible to obtain an accurate estimate of upper shelf energy in only the 12 thick A350-LF3 forging (Fig. 7). However, the mill sheets reported Charpy energies ranging from 153 to 162 ft-lb at -20 °F in the two A508-4B forgings. Based on Figs 4 and 5, this temperature would appear to be well on the upper shelf for this material.

A comparison of Charpy and NDTT results reveals an anomaly in the A508-4A and 4B data. According to the NDTT results, the 4A forgings are tougher than the 4B forgings; NDTT values range from -210 to -250 °F for the 4A forgings and from -170 to -220 °F for the 4B forgings. However, the Charpy results exhibit the opposite trend, in that the CVN transition temperatures for the 4A forgings are considerably higher than the 4B forgings. As stated above, the NDTT results for the A508 forgings are suspect because arrests were occurring in the HAZ rather than the parent metal. This is explored further in the *Discussion*.

METALLOGPAHIC EXAMINATION

Figures 8 to 10 show the microstructures of the various forgings and thickness locations. Ferrite sizes are reported in Table 6 for the cases where such measurements were possible.

When low carbon alloy steels are tempered at high temperatures (600 - 700 °C) the microstructral changes which can be observed with light microscopy are typically as follows(2). In early stages of tempering, the microstructure is indistinguishable from the as-quenched lath matensite structure. Even in relatively advanced stages of tempering, the steel retains its packet morphology with parallel subunits. The main observable changes are a decrease in the lath spacing, and precipitation of spherical carbides at prior austenitic grain boundaries and within packets. A fully tempered microstructure consists of equiaxed ferrite grains and spherical carbides. Many of these phenomena can be observed in Figs. 8 to 10.

Figures 8a to 8e are photomicrographs of the A508-4B microstructure at the various locations in the two forgings. In the 8 in forging, (Figs 8a and 8b), the microstructure does not change significantly through the thickness. The microstructure consists of well tempered martensite. There is little or no evidence of equiaxed ferrite nucleation. However, the microstructure of the

12 in forging (Figs 8c, 8d, 8e) does contain a few ferrite grains. This indicates that the thicker forging was tempered more thoroughly. As was the case for the 8 in forging, there are little or no observable differences in microstructure through the thickness of the 12 in forging.

In Fig. 9a, which shows the microstructure of the center of the 8 in A508-4B forging, some equiaxed ferrite grains have begun to form. In the outer region of this forging (Fig. 9b), however, the tempering process appears to be at an earlier stage since only 1 or 2 ferrite grains can be seen in the photograph. Figures 9c, 9d and 9e are all similar to Fig. 9b, in that the microstructure is predominantly tempered martensite, with evidence of the formation of a few equiaxed ferrite grains.

The microstructure of the A350-LF3 forgings (Figs 10a to 10e) indicates a very advanced stage of tempering. Plane A of the 8 in forging (Fig. 10a) is almost entirely equiaxed ferrite with small spherical carbides dispersed throughout the microstructure. Note that the carbide particles are grouped together along straight lines, indicating the former location of austenite grain boundaries and packet boundaries. Plane B has a similar microstructure to plane A, except that there is still evidence of the martensitic packet structure. The 12 in forging (Figs 10c, 10d and 10e) is more thoroughly tempered than the 8 in forging. A few inclusions can be seen in Figs. 10a to 10e, while virtually no inclusions were observed in the A508-4A or -4B steel. This is not surprising, given that the A350-LF3 steel has significantly higher S content than the other two materials (see Table 2).

Several trends emerge from the microscopic examination. First, the center of a forging tends to be more thoroughly tempered than the outer regions. In addition, the 12 in forging was more thoroughly tempered than the 8 in forging in two out of three cases. This implies that regions which are less severely quenched (i.e. the thicker forgings and the interior region of a given forging) tend to undergo more rapid.transformation upon tempering. Coincident with a well tempered microstructure is low toughness, both in terms of NDTT and CVN energy. When the microstructure is a finely spaced tempered martensite, cleavage fracture is difficult because a propagating crack must change direction each time it encounters a packet boundary. As tempering progresses, the average packet diameter increases and toughness decreases. When equiaxed ferrite grains form, toughness decreases still further because the microstructure is considerably coarser than the packet structure which existed previously (see Figs. 8 to 10).

DISCUSSION

As expected, this study showed that toughness can vary through the thickness of a thick section. Thus, it important to take this into account when setting

toughness guidelines for a particular application. The previous section discussed some of the metallurgical reasons for inhomogeneity in toughness.

Although the NDTT results give information about the relative toughness of the various materials and locations, the absolute values are suspect for two reasons: 1) most cracks arrested in the HAZ rather than the parent metal, and 2) the the specimens were tested with a nonstandard deflection height. These two factors would have opposite effects on the measured NDTT. Increasing the deflection height will tend to increase NDTT because more energy is available to drive the cleavage crack through the specimen. When the HAZ is tougher than the parent metal, the measured NDTT will decrease because the drop weight test will measure the arrest properties of the HAZ.

The effect of deflection height is probably small because the transition is relatively steep for these materials. Increasing the deflection height by 25 percent is roughly equivalent to a 25 percent change in CVN energy. For example, consider the CVN transition curve for Plane A of the A508-4A steel (Fig. 2). The 60 ft-lb transition temperature occurs at approximately -38 °F while the 75 ft-lb transition occurs at -18 °F. Thus, the nonstandard deflection height probably increased the measured NDTT values by roughly 20 °F.

The HAZ microstructural effect is potentially very serious. Moreover, there is little that can be done about it, aside from significantly increasing the heat input to the welding process in order to produce more brittle HAZs. Of the two competing effects present in this study, the HAZ effect probably dominated, as discussed below.

Satoh, et. al. (3) have developed a correlation between the NDTT and the 50 ft-lb transition temperature. Their correlation, in units of Fahrenheit, is given by

$$NDTT = 0.7\, T_{50\ ft\text{-}lb} - 27.0 \qquad [1]$$

We used Eq. [1] to estimate expected NDTT values based on the CVN data. Predicted and measured NDTTs are given in Table 7 and Fig. 11. The measured NDTT values for the A508-4A forging are significantly below what would be expected from the Charpy data. This indicates that the HAZ toughness dominated these drop weight tests. Had we been able to measure the true NDTT of the parent metal, it probably would not have met the NRC requirements(1). The measured and predicted values for the A508-4B steel agree very closely. This is consistent with experimental observations. All of the specimens in which arrest occurred well into the parent metal were made of this material. The HAZ and parent metal of the A508-4B steel apparently had similar toughness; the NDTT tests were indicative of the parent metal properties in this case. The measured NDTT values in the A350-LF3 steel are slightly lower than predicted from Eq. [1].

Figure 11 and Table 7 indicate that the HAZ properties tended to dominate the NDTT results, particularly in the case of the A508-4A steel. There was poor correlation between the CVN properties and NDTT values in this material. The main difference between this steel and the other two materials is the Cr content, which is highest in the 4A material. (The parent metal microstructures of the three steels are somewhat different, but this should have little effect on the HAZ that is produced by welding.) Apparently , the presence of Cr is conducive to producing tough HAZs. This is desirable from a structural standpoint, but makes it difficult or impossible to perform meaningful tests according to E 208.

CONCLUSIONS

1. The toughness of low alloy steel forgings tends to decrease with section thickness and tends to be lower in the center of thick sections. The apparent metallurgical cause for this phenomenon is that lower quench rates result in faster tempering rates which in turn result in a coarser microstructure with lower toughness.

2. Chemical analyses commissioned by the authors indicates a significantly lower Cr content in the A508-4B than was reported by the steel mill. If the most recent analyses are correct, the material does not meet the requirements of ASTM A508 Class 4.

3. The NDTT results tended to be lower than would be expected from the Charpy data. This was particularly true for the A508-4A steel. The NDTT values were artificially low because the drop weight tests were actually measuring the arrest properties of the heat-affected zone, which tended to be tougher than the parent metal. The use of a nonstandard deflection height may have partially offset this effect.

REFERENCES

1. Anon, "Fracture Toughness Criteria for Ferritic Steel Shipping Containers with a Wall Thickness Greater Than Four Inches (0.1 m)." Draft Regulatory Guide and Value/ Impact Statement, U.S. Nuclear Regulatory Commission, June 1986.

2. Krauss, G., *Principles of Heat Treatment of Steel,* American Society for Metals, Metals Park, Ohio, 1980.

3. Satoh, M, Funada, T., and Tomimatsu, M., "Evaluation of Valid Nil-Ductility Transition Temperatures for Nuclear Vessel Steels." In ASTM STP 919, 1986, pp. 16-33.

TABLE 1. Mechanical properties of the steel forgings as reported on the mill sheets

Material	Yield Strength (ksi)	Tensile Strength (ksi)	Percent Elongation	Percent Reduction in Area
A508-4A (8 in)	102	117	25.5	73.3
A508-4A (12 in)	106	119	25.5	71.6
A508-4B (8 in)	85.5	105	29.0	76.1
A508-4B (12 in)	88.5	107	31.5	75.9
A350-LF3 (8 in)	65.5	86.5	30.0	69.7
A350-LF3 (12 in)	65.5	86.5	60.0	69.7

TABLE 2a. Chemical composition of the A508-4A forgings.

	COMPOSITION, (weight percent)										
Sample	C	Mn	P	S	Si	Ni	Cr	Mo	V	Nb	Cu
A	0.17	0.195	0.02	0.01	0.21	2.88	1.49	0.45	0.003	0.01	0.147
B	0.18	0.199	0.02	0.01	0.21	2.94	1.48	0.46	0.003	0.01	0.150
C	0.18	0.194	0.02	0.01	0.21	2.83	1.51	0.45	0.003	0.01	0.145
D	0.19	0.205	0.02	0.01	0.21	3.02	1.56	0.48	0.003	0.01	0.153
E	0.18	0.199	0.02	0.01	0.22	2.90	1.54	0.46	0.003	0.01	0.149
Mill 1	0.17	0.23	0.01	0.001	0.25	3.20	1.64	0.52	0.006	(not measured)	
Mill 2	0.17	0.23	0.010	0.001	0.25	3.21	1.65	0.52	0.006	(not measured)	
Spec.	<0.23	0.20-0.40	<0.20	<0.20	0.15-0.40	2.75-3.90	1.50-2.00	0.40-0.60	<0.03		

TABLE 2b. Chemical composition of the A508-4B forgings.

	COMPOSITION, (weight percent)										
Sample	C	Mn	P	S	Si	Ni	Cr	Mo	V	Nb	Cu
A	0.18	0.189	0.02	<.01	0.22	3.01	1.16	0.44	0.003	0.01	0.151
B	0.18	0.186	0.02	<.01	0.22	2.96	1.13	0.44	0.003	0.01	0.148
C	0.18	0.185	0.02	<.01	0.22	2.89	1.24	0.43	0.003	0.01	0.148
D	0.19	0.192	0.02	0.01	0.22	2.99	1.24	0.45	0.003	0.01	0.153
E	0.18	0.184	0.02	<.01	0.22	2.92	1.10	0.43	0.003	0.01	0.148
Mill 1	0.17	0.23	0.01	0.001	0.25	3.20	1.64	0.52	0.006	(not measured)	
Mill 2	0.17	0.23	0.010	0.001	0.25	3.21	1.65	0.52	0.006	(not measured)	
Spec.	<0.23	0.20-0.40	<0.20	<0.20	0.15-0.40	2.75-3.90	1.50-2.00	0.40-0.60	<0.03		

TABLE 2c Chemical composition of the A530-LF3 forgings.

	COMPOSITION, (weight percent)										
Sample	C	Mn	P	S	Si	Ni	Cr	Mo	V	Nb	Cu
A	0.16	0.780	0.02	0.03	0.16	3.16	0.162	0.02	0.030	<.01	0.207
B	0.16	0.780	0.02	0.03	0.16	3.14	0.163	0.02	0.032	<.01	0.206
C	0.16	0.779	0.02	0.03	0.16	3.14	0.162	0.02	0.032	<.01	0.204
D	0.17	0.800	0.03	0.04	0.16	3.15	0.163	0.02	0.032	<.01	0.209
E	0.15	0.778	0.02	0.03	0.16	3.18	0.164	0.02	0.031	<.01	0.207
Mill	0.15	0.81	0.019	0.025	0.21	3.36	.....(not measured).....				
Spec.	<0.20	<0.90	<0.035	<0.040	0.20-0.35	3.25-3.75					

TABLE 3. Nil-ductility transition temperature data for the steel forgings.

Material	Thickness (in)	Location*	NDTT, (°F)+
A508-4A	8	Plane A	-210
	"	Plane B	-250
	12	Plane C	-230
	"	Plane D	-250
	"	Plane E	-250
A508-4B	8	Plane A	-200
	"	Plane B	-220
	12	Plane C	-170
	"	Plane D	-190
	"	Plane E	-190
A350-LF3	8	Plane A	-80
	"	Plane B	-100
	12	Plane C	-50
	"	Plane D	-60
	"	Plane E	-60

*See Fig. 1

+P2 specimens tested with nonstandard deflection height of 0.075 in.

Table 4a. Results of individual drop weight tests on A508-4A steel.

PLANE	TEMPERATURE, °F									
	-260 °F	-250 °F	-240 °F	-230 °F	-220 °F	-210 °F	-200 °F	-190 °F	-180 °F	-170 °F
A					●	⊗ ●	○ ○			⊗
B		●	○ ○	○	○					
C				●	○ ○	○				
D	●	●	○ ○							
E	●	○ ●	○ ○							

● BREAK ○ NO BREAK ⊗ NO TEST

Table 4b. Results of individual drop weight tests on A508-4B steel.

PLANE	TEMPERATURE, °F									
	-220 °F	-210 °F	-200 °F	-190 °F	-180 °F	-170 °F	-160 °F	-150 °F	-140 °F	-130 °F
A		●	●	○ ○ ●	●	○ ○				
B	●	○ ○ ○ ●	○							
C						● ○	○ ○	○		○
D				●	○ ○	○				
E			●	○ ●	○ ○			○		

● BREAK ○ NO BREAK ⊗ NO TEST

Table 4c. Results of individual drop weight tests on A350-LF3 steel.

PLANE	TEMPERATURE, °F									
	-130 °F	-120 °F	-110 °F	-100 °F	-90 °F	-80 °F	-70 °F	-60 °F	-50 °F	-40 °F
A	●				●	○ ●	○ ○		○	
B				●	○ ○	○		○		
C									●	○ ⊠ ○
D						● ●	●	○ ●	○ ○	
E						●	○ ●	○ ⊠ ●	○ ○	

● BREAK ○ NO BREAK ⊠ NO TEST

TABLE 5a. Charpy data for the A508-4A forgings

Temp (A) (°F)	CVN(A) (Ft-lb)	Temp(B) (°F)	CVN(B) (Ft-lb)	Temp(C) (°F)	CVN(C) (Ft-lb)	Temp(D) (°F)	CVN(D) (Ft-lb)	Temp(E) (°F)	CVN(E) (Ft-lb)
-167.00	13.000	-271.00	16.000	-199.00	8.5000	-195.00	6.5000	-188.00	6.5000
-121.00	14.500	-225.00	25.000	-170.00	7.0000	-151.00	16.500	-154.00	13.500
-90.000	18.000	-200.00	39.500	-134.00	16.500	-127.00	12.000	-144.00	20.500
-84.000	32.500	-184.00	23.000	-92.000	16.000	-107.00	13.500	-134.00	31.000
-78.000	54.500	-178.00	22.500	-79.000	27.500	-101.00	24.000	-115.00	41.000
-71.000	51.000	-172.00	58.000	-66.000	54.000	-95.000	31.000	-109.00	67.500
-65.000	42.000	-169.00	75.000	-61.000	31.500	-78.000	31.000	-105.00	38.500
-53.000	39.500	-165.00	79.500	-53.000	35.500	-70.000	38.000	-99.000	29.000
-40.000	57.000	-157.00	70.500	-42.000	52.500	-60.000	60.500	-94.000	72.500
-25.000	62.000	-152.00	31.500	-34.000	49.500	-51.000	77.000	-90.000	25.000
-17.000	77.500	-140.00	85.500	-26.000	97.000	-45.000	64.000	-89.000	54.000
-10.000	97.000	-131.00	65.000	-18.000	116.00	-40.000	82.000	-83.000	61.500
0.0000	83.500	-129.00	29.000	-11.000	76.500	-36.000	99.000	-77.000	82.000
7.0000	96.500	-125.00	57.500	-6.0000	116.50	-26.000	113.50	-73.000	107.50
13.000	114.50	-116.00	120.00+	4.0000	112.00	-13.000	112.50	-68.000	120.00+
31.000	114.50	-109.00	120.00+	13.000	120.00+	4.0000	120.00+	-54.000	116.50

TABLE 5b. Charpy data for the A508-4B forgings.

Temp (A) (°F)	CVN(A) (Ft-lb)	Temp(B) (°F)	CVN(B) (Ft-lb)	Temp(C) (°F)	CVN(C) (Ft-lb)	Temp(D) (°F)	CVN(D) (Ft-lb)	Temp(E) (°F)	CVN(E) (Ft-lb)
-283.00	13.000	-306.00	7.0000	-250.00	26.500	-263.00	17.000	-276.00	40.500
-269.00	14.500	-282.00	14.500	-218.00	12.000	-224.00	26.500	-264.00	56.500
-253.00	8.5000	-280.00	56.000	-200.00	15.000	-201.00	40.000	-261.00	16.500
-245.00	18.500	-273.00	43.000	-182.00	39.000	-184.00	64.000	-248.00	35.000
-238.00	12.000	-269.00	60.500	-169.00	12.500	-178.00	66.500	-241.00	57.000
-229.00	108.50	-266.00	55.000	-165.00	120.00	-176.00	70.000	-238.00	77.500
-218.00	53.500	-259.00	28.000	-160.00	53.500	-167.00	66.500	-229.00	40.000
-208.00	94.500	-255.00	65.000	-159.00	70.000	-163.00	76.000	-226.00	111.00
-205.00	55.500	-250.00	71.000	-157.00	79.000	-158.00	67.500	-223.00	39.500
-200.00	120.00+	-239.00	85.000	-147.00	55.000	-153.00	53.000	-217.00	82.500
-193.00	88.500	-230.00	90.000	-144.00	44.500	-150.00	48.500	-210.00	70.500
-185.00	120.00+	-223.00	90.000	-143.00	64.000	-142.00	83.000	-205.00	112.50
-179.00	99.500	-220.00	114.50	-140.00	110.50	-137.00	88.500	-197.00	117.50
-171.00	120.00+	-192.00	120.00+	-138.00	117.50	-134.00	84.000	-168.00	108.00
-159.00	114.50	-171.00	116.00	-127.00	120.00+	-128.00	113.50	-161.00	118.00
-108.00	120.00+	-155.00	120.00+	-114.00	116.00	-120.00	120.00+	-138.00	116.00

TABLE 5c. Charpy data for the A350-LF3 forgings

Temp (A) (°F)	CVN(A) (Ft-lb)	Temp(B) (°F)	CVN(B) (Ft-lb)	Temp(C) (°F)	CVN(C) (Ft-lb)	Temp(D) (°F)	CVN(D) (Ft-lb)	Temp(E) (°F)	CVN(E) (Ft-lb)
-110.00	13.000	-108.00	15.500	-109.00	7.0000	-109.00	10.000	-108.00	8.5000
-95.000	12.000	-92.000	24.000	-95.000	10.000	-95.000	15.500	-95.000	11.000
-81.000	30.000	-81.000	30.000	-69.000	7.0000	-57.000	18.500	-81.000	12.000
-69.000	33.000	-69.000	39.000	-44.000	21.500	-44.000	27.500	-70.000	15.500
-57.000	54.000	-57.000	45.000	-32.000	21.500	-25.000	31.500	-57.000	23.000
-44.000	48.500	-44.000	49.500	-26.000	38.000	-7.0000	29.500	-26.000	21.500
-33.000	47.000	-27.000	48.500	-10.000	29.500	7.0000	37.500	-4.0000	29.000
-26.000	75.500	-17.000	46.000	-7.0000	18.000	22.000	50.000	15.000	34.000
-17.000	67.500	-12.000	58.500	0.0000	36.000	32.000	56.000	39.000	50.000
-7.0000	72.000	-7.0000	86.000	7.0000	53.000	37.000	63.000	57.000	66.500
15.000	88.000	0.0000	74.000	22.000	40.500	41.000	71.500	67.000	55.000
28.000	114.50	7.0000	84.500	41.000	57.500	47.000	69.500	70.000	54.000
41.000	116.50	15.000	69.000	57.000	65.000	57.000	67.500	76.000	81.500
57.000	107.00	41.000	102.50	76.000	82.000	76.000	82.500	100.00	81.000
74.000	120.00+	57.000	120.00+	100.00	84.500	92.000	84.000	120.00	85.500
75.000	120.00+	78.000	120.00+	122.00	75.500	124.00	80.500	136.00	78.000

TABLE 6. Ferrite grain size for the low alloy steel forgings as a function of position in thickness.

Alloy	Thickness Position*	Average Grain Diameter, μm
A508-4A	Plane A	----
	Plane B	----
	Plane C	12.7
	Plane D	----
	Plane E	----
A508-4B	Plane A	10.3
	Plane B	----
	Plane C	----
	Plane D	----
	Plane E	----
A350-LF3	Plane A	13.8
	Plane B	12.6
	Plane C	17.3
	Plane D	11.8
	Plane E	10.2

TABLE 7. Comparison of NDTT with values estimated from the Satoh, et. al. equation(3).

Alloy	Thickness Position*	Measured NDTT+ (°F)	Predicted NDTT (°F)
A508-4A	Plane A	-210	-62
	Plane B	-250	-139
	Plane C	-230	-63
	Plane D	-250	-80
	Plane E	-250	-101
A508-4B	Plane A	-200	-180
	Plane B	-220	-211
	Plane C	-170	-146
	Plane D	-190	-160
	Plane E	-190	-201
A350-LF3	Plane A	-80	-56
	Plane B	-100	-56
	Plane C	-50	+8
	Plane D	-60	-13
	Plane E	-60	+8

*See Fig. 1

+P2 specimens tested with a nonstandard deflection height of 0.075 in.

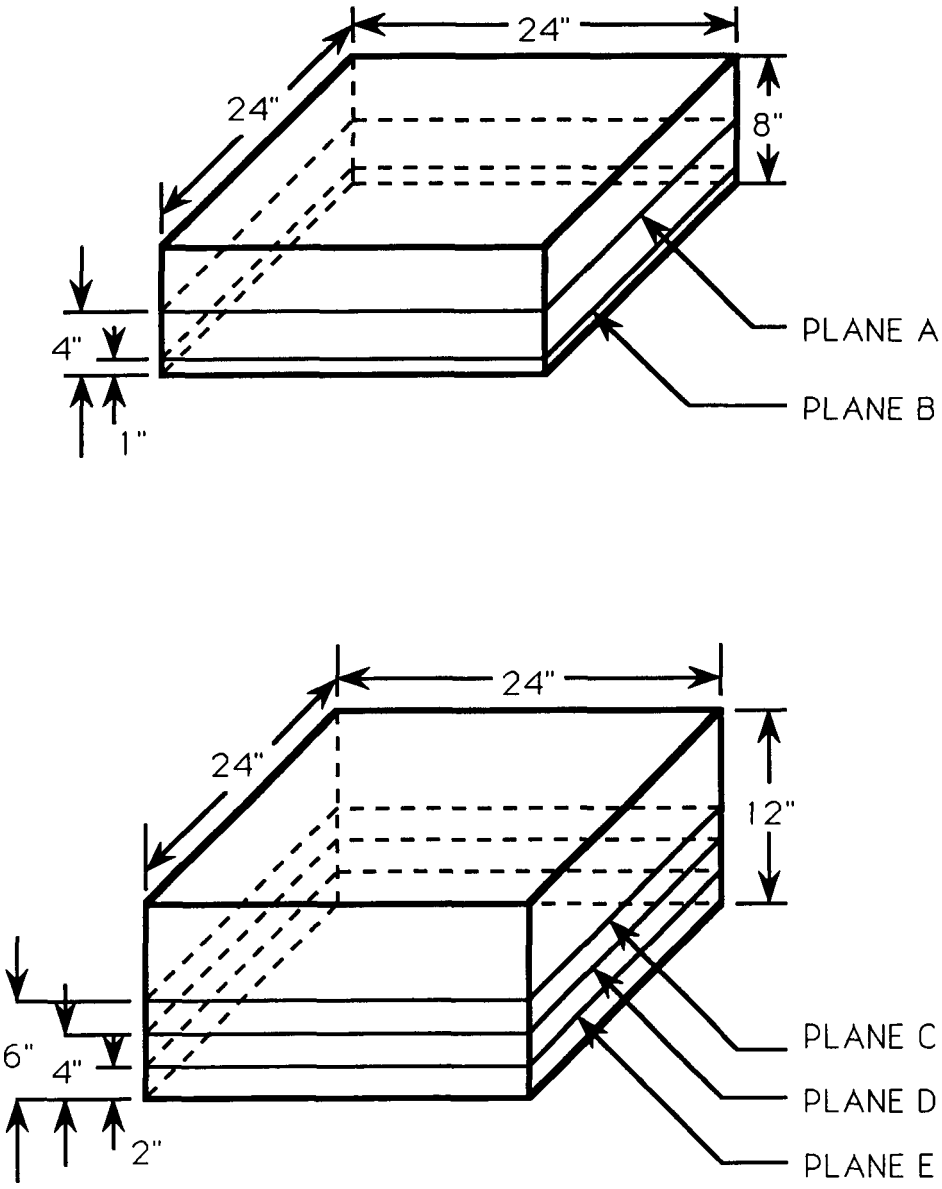

FIG. 1. Drawing of the 8 in and 12 in thick forgings which shows the locations from which specimens were extracted.

FIG. 2. Charpy data for the 8 in thick A508-4A forging.

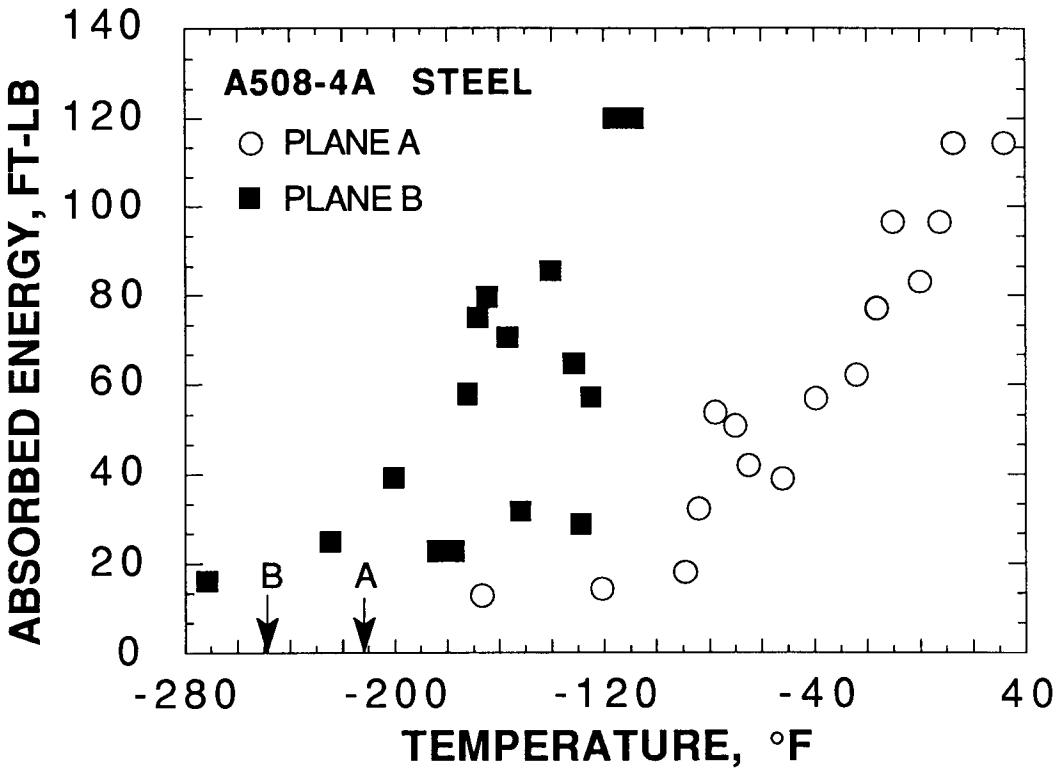

Fig. 3. Charpy data for the 12 in thick A508-4A forging.

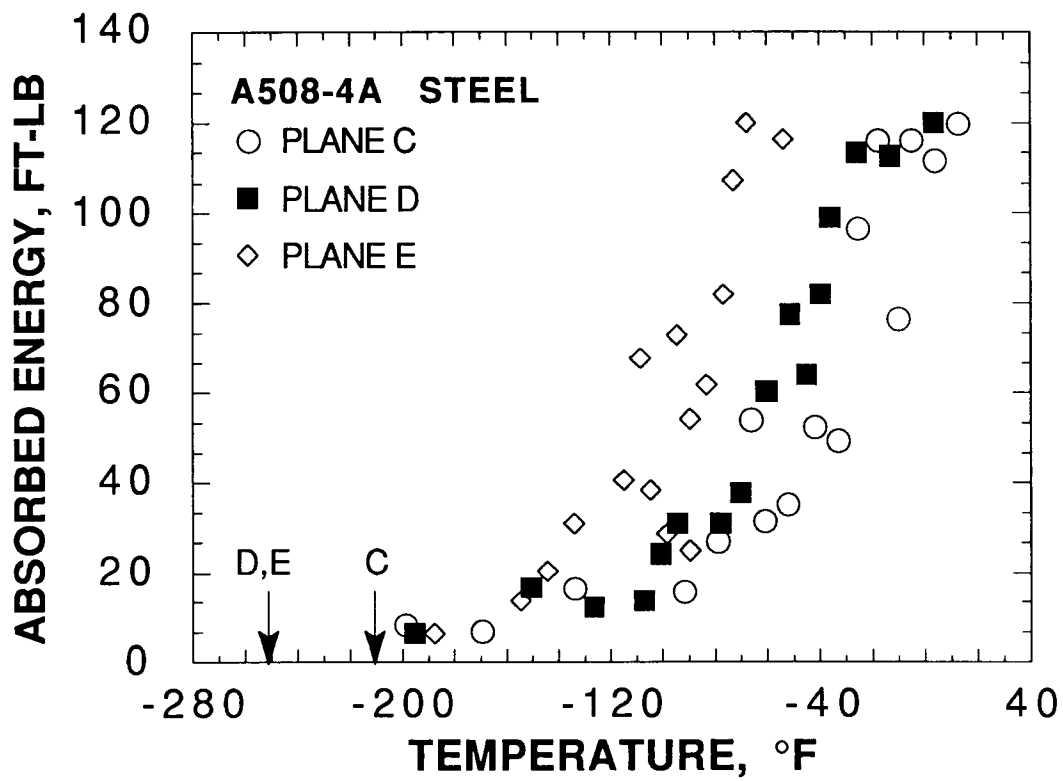

FIG. 4. Charpy data for the 8 in thick A508-4B forging.

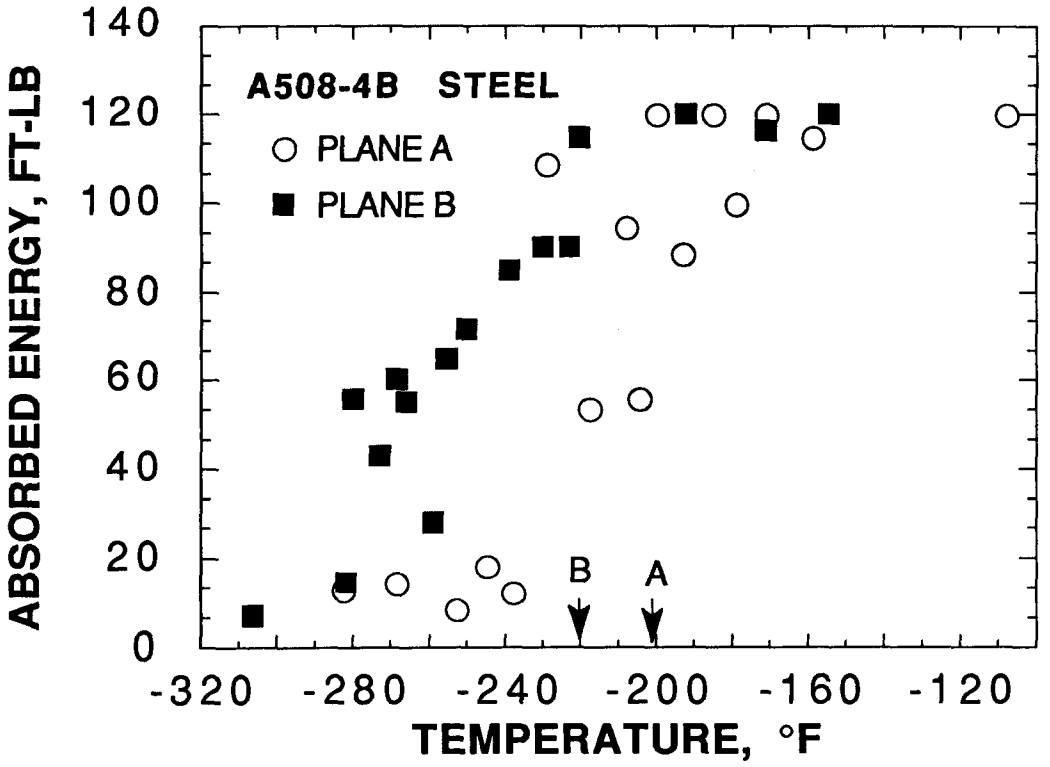

FIG. 5. Charpy data for the 12 in thick A508-4B forging.

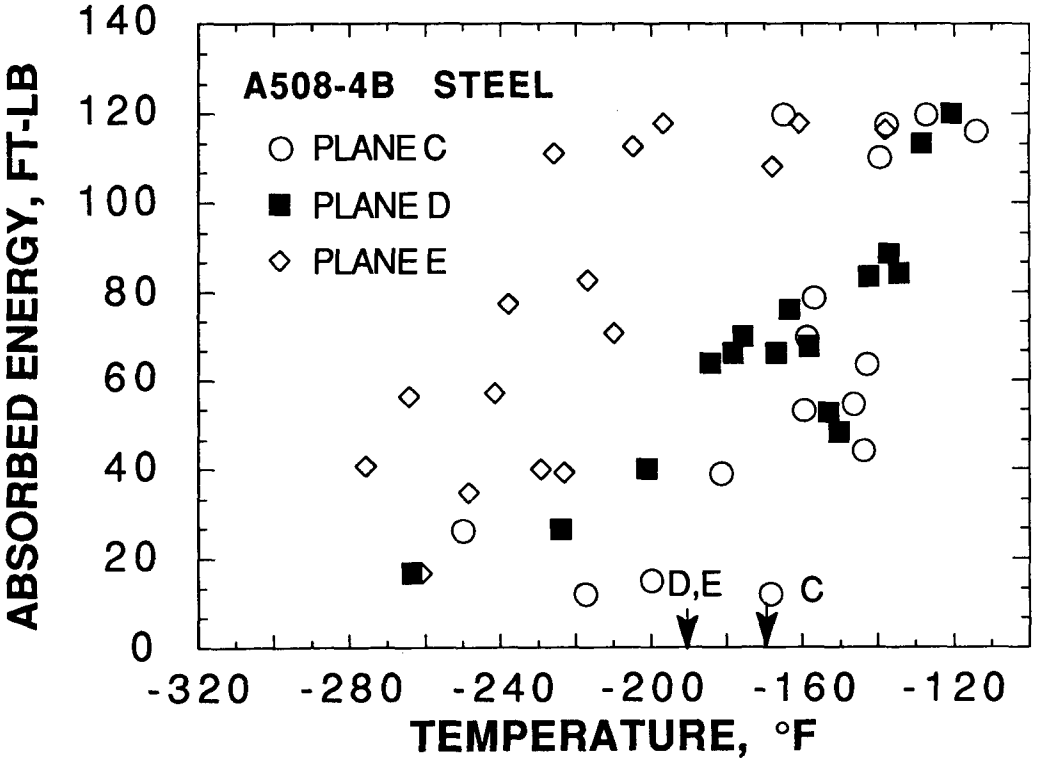

FIG. 6. Charpy data for the 8 in thick A350-LF3 forging.

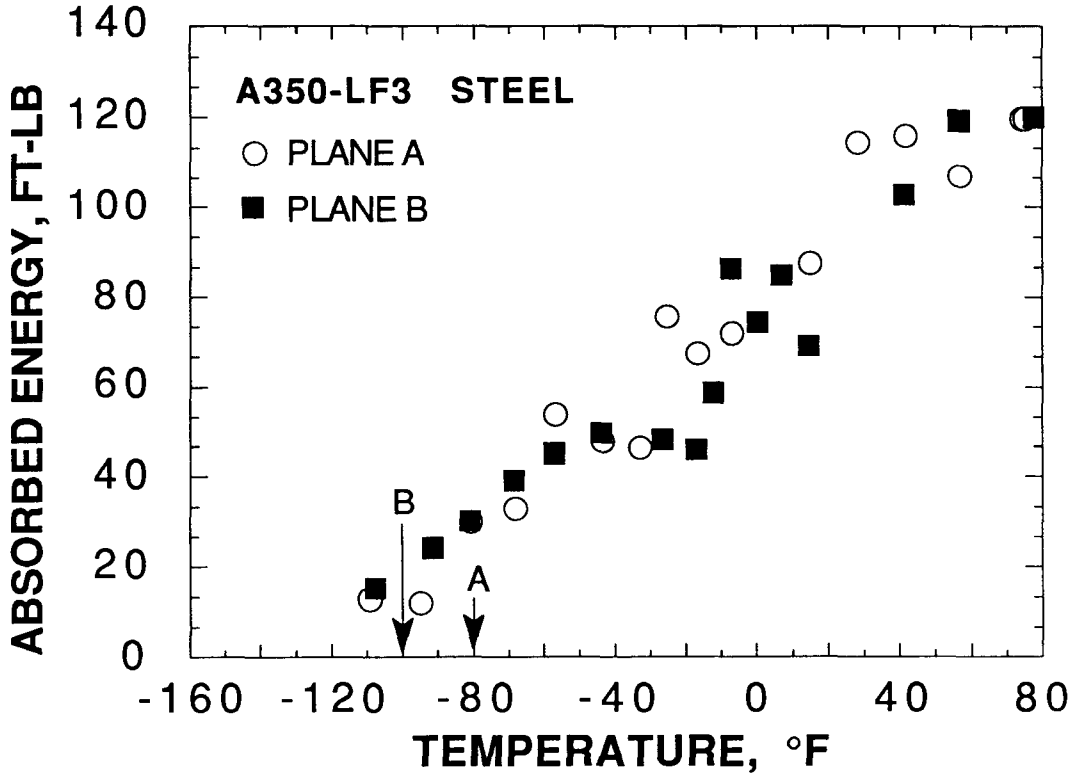

FIG. 7. Charpy data for the 12 in thick A350-LF3 forging.

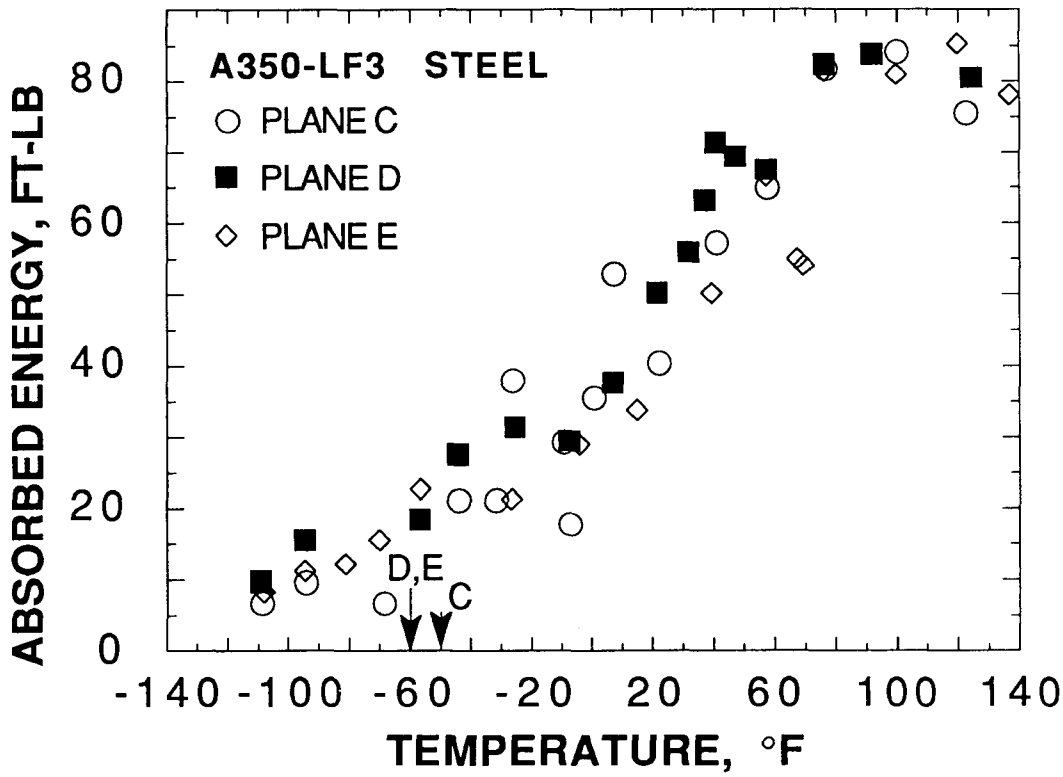

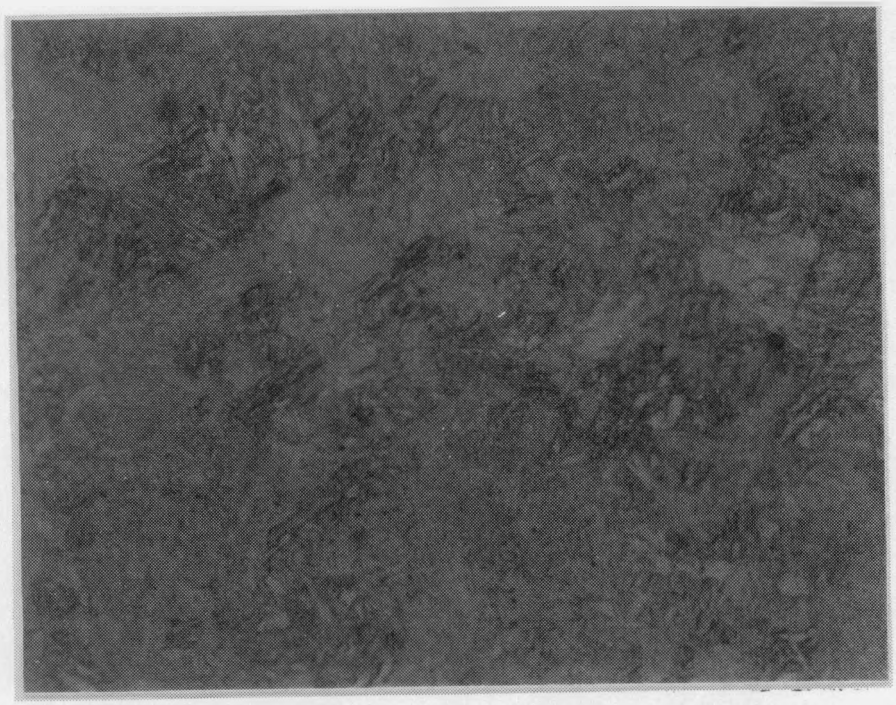

Fig. 8a. Microstructure of Plane A of the A508-4A steel. 400X magnification.

Fig. 8b. Microstructure of Plane B of the A508-4A steel. 400X magnification.

Fig. 8c. Microstructure of Plane C of the A508-4A steel. 400X Magnification.

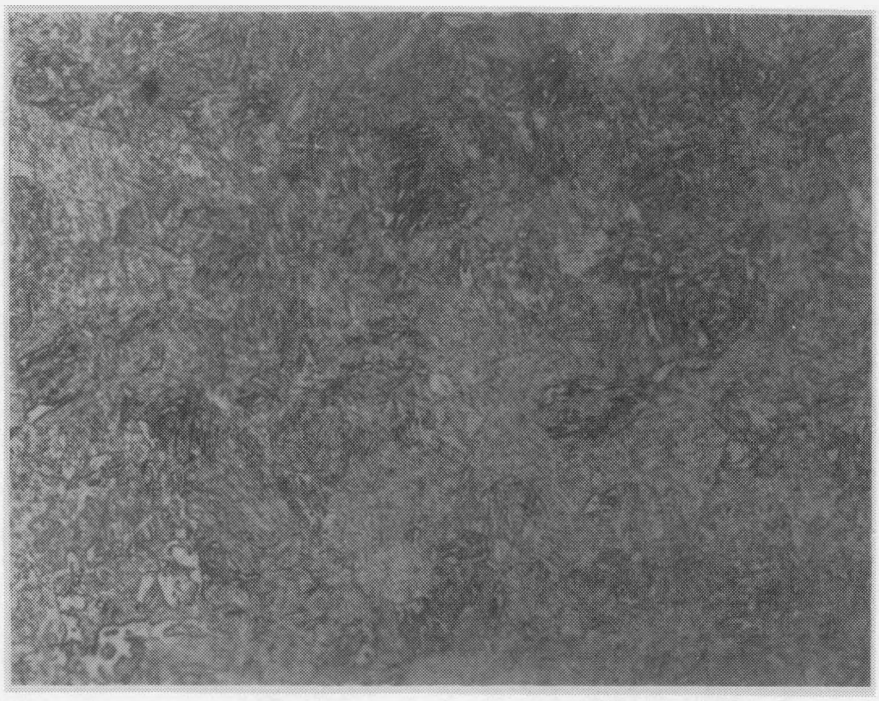

Fig. 8d. Microstructure of Plane D of the A508-4A steel. 400X Magnification.

Fig. 8e. Microstructure of Plane E of the A508-4A steel. 400X Magnification.

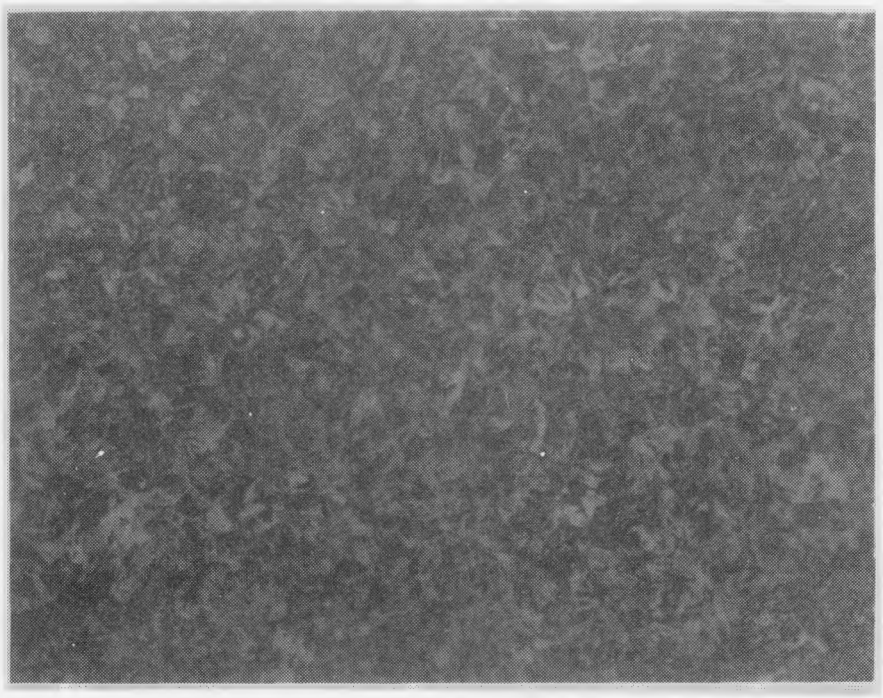

Fig. 9a. Microstructure of Plane A of the A508-4B steel. 400X magnification.

Fig. 9b. Microstructure of Plane B of the A508-4B steel. 400X magnification.

Fig. 9c. Microstructure of Plane C of the A508-4B steel. 400X Magnification.

Fig. 9d. Microstructure of Plane D of the A508-4B steel. 400X Magnification.

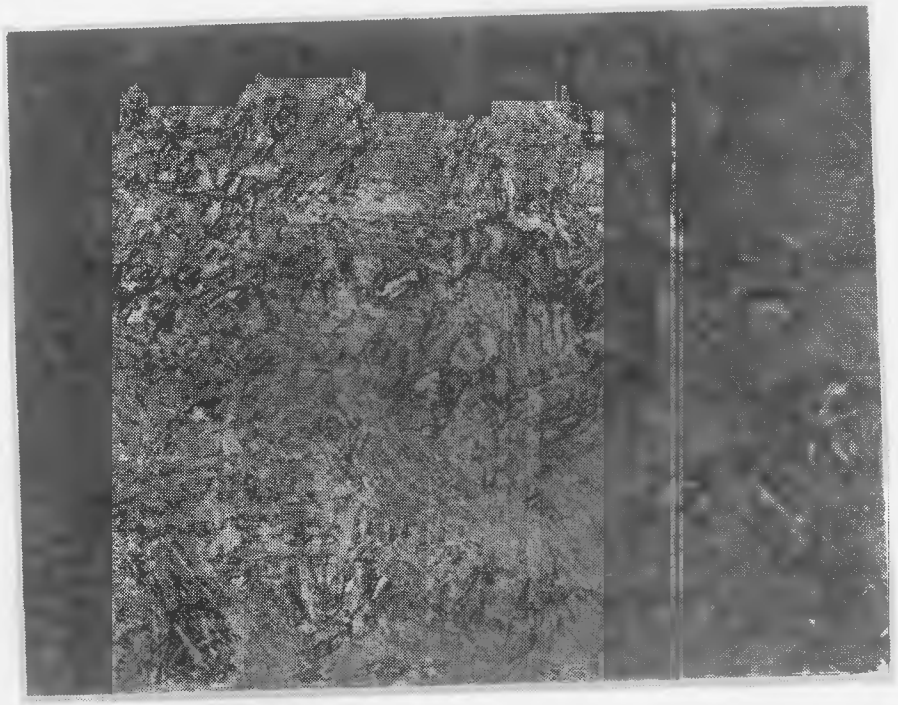

Fig. 9e. Microstructure of Plane E of the A508-4B steel. 400X Magnification.

Fig. 10a. Microstructure of Plane A of the A350-LF3 steel. 400X magnification.

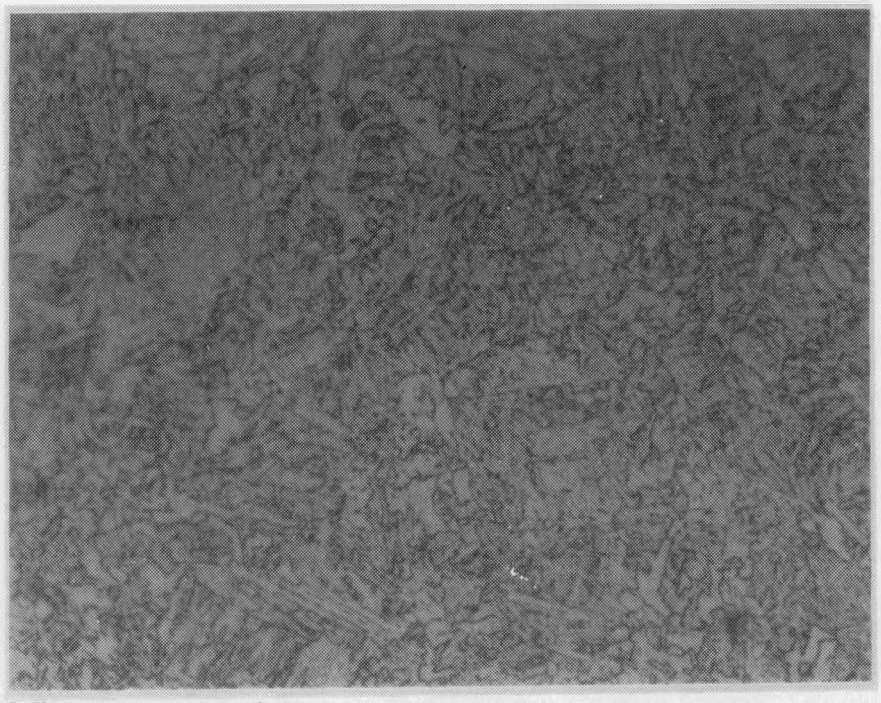

Fig. 10b. Microstructure of Plane B of the A350-LF3 steel. 400X magnification.

Fig. 10c. Microstructure of Plane C of the A350-LF3 steel. 400X Magnification.

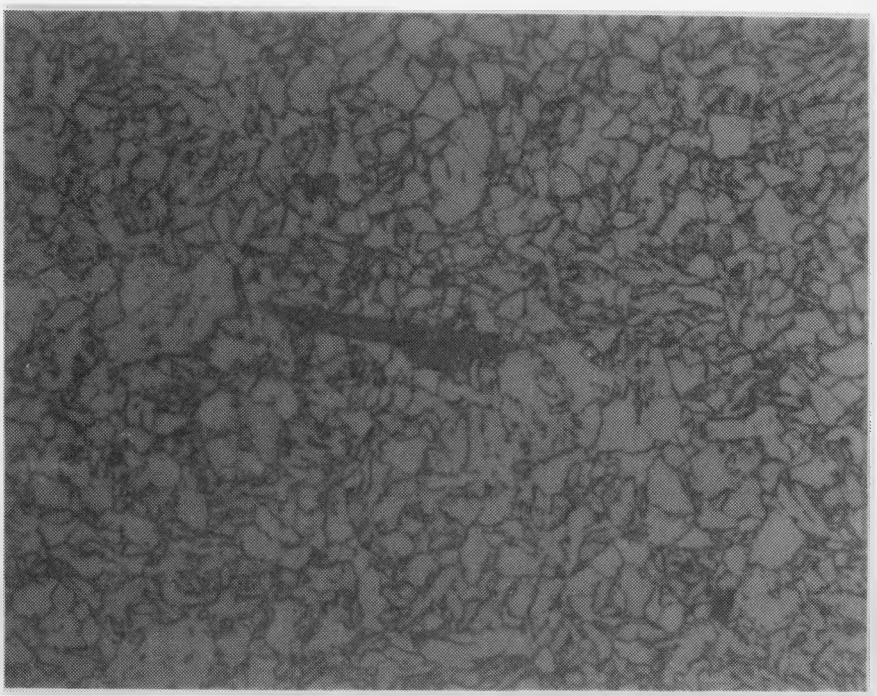

Fig. 10d. Microstructure of Plane D of the A350-LF3 steel. 400X Magnification.

Fig. 10e. Microstructure of Plane E of the A350-LF3 steel. 400X Magnification.

FIG. 11. Comparison of measured NDTT with NDTT estimated from CVN transition curves.